arXiv:1702.07565v1 [quant-ph] 24 Feb 2017

Optically driven ultra-stable nanomechanical rotor

Stefan Kuhn,[1,*] Benjamin A. Stickler,[2] Alon Kosloff,[3] Fernando Patolsky,[3] Klaus Hornberger,[2] Markus Arndt,[1] and James Millen[1]

[1] *University of Vienna, Faculty of Physics, VCQ, Boltzmanngasse 5, 1090 Vienna, Austria*
[2] *University of Duisburg-Essen, Lotharstraße 1, 47048 Duisburg, Germany*
[3] *School of Chemistry, Tel-Aviv University, Ramat-Aviv 69978, Israel*

Nanoscale mechanical oscillators are sensitive to a wide range of forces, and are the subject of studies into fundamental quantum physics [1]. They can be used for mass detection at the single proton level [2], position measurements to the quantum limit [3, 4], and they have found application in genetics, proteomics, microbiology and studies of DNA [5]. Their sensitivity is limited by dissipation to the environment, which reduces the mechanical quality factor $Q_{\rm m}$. Here we realize a nanomechanical rotor with remarkably high $Q_{\rm m}$, by optically levitating a silicon nanorod and periodically driving its rotation with circularly polarized light [6–8]. We frequency-lock the nanorod's motion to the periodic drive, resulting in ultra-stable rotations, with a stability close to that of the drive. While operating at room temperature, and gas pressures of a few millibar, our system exhibits an effective $Q_{\rm m}$ of 10^{11}, and a $Q_{\rm m}$-frequency product of 10^{17} Hz, three orders of magnitude greater than measured in any other experiment [9, 10]. This frequency stability yields an unprecedentedly high room temperature torque sensitivity of 0.24 zNm [11] and a relative pressure sensitivity of 0.3 %. In addition, the external drive allows us to tune the rotational frequency by almost 10^{12} linewidths, and the ability to make local phase sensitive measurements allows real-time readout, offering a new paradigm of flexibility in sensing applications.

Nanomechanical oscillators have great technological utility [12] due to their extreme sensitivity to external forces [13–15], torques [11], acceleration [16], charge [17], and added mass [2]. Devices with mechanical quality factors of $Q_{\rm m} \simeq 10^8$ have been realized [9, 10], and many systems can be improved by parametrically driving the oscillator [18–20]. However, their performance is eventually limited by environmental dissipation through material stresses [21]. A well established method to decrease coupling to the environment is to levitate a micro- or nano-particle in an external field in vacuum [8, 22–26]. Here, the performance is only limited by laser power fluctuations and collisional damping by residual gas particles. In levitated systems, $Q_{\rm m}$ of 10^8 have been measured [27], allowing force sensing at the zepto-Newton level [15].

In this work, we achieve ultra-high $Q_{\rm m}$ rotations by periodically driving the rotation of an optically levitated silicon nanorod. We observe locking of the nanorotor to the periodic drive, such that its mean rotation frequency $f_{\rm r}$ becomes independent of pressure or laser power fluctuations. Thereby, we overcome the limitations of material stress, collisional damping and even the necessity to work in ultra high vacuum, to achieve an unprecedentedly high torque sensitivity of sub-zepto Nm at room temperature and millibar pressures.

We levitate a nanofabricated silicon nanorod in the standing light wave formed by two counterpropagating laser beams, and track its motion by monitoring the scattered light, see Fig.1a and Methods. When the laser is linearly polarized, the nanorod is harmonically trapped in an antinode of the standing wave and aligned with the field polarization. When the laser is circularly polarized, the scattered light exerts a torque [6–8] and propels the nanorod in the plane orthogonal to the beam axis, while its centre-of-mass remains trapped [8]. The maximum rotation frequency of the rod is determined by its size, the pressure, and the laser intensity [8]. Collisions with gas particles and centre-of-mass excursions into regions of different light intensity give rise to a broad distribution of rotational frequencies [8], as shown by the blue curve in Fig. 1c.

However, if the rod is driven by periodically switching the laser polarization between linear and circular, the rod can frequency-lock to this modulation, leading to a sharp peak in the power spectral density (PSD) of the scattered light (Fig. 1b). The locked rotation peak is eleven orders of magnitude narrower than in the unlocked case (see Fig.1c) and when locked, the frequency can be continuously tuned over a range of 10^{12} linewidths (Fig. 4a).

In order to characterize the frequency-locked rotation, we drive the nanorod with frequency $f_{\rm d} = 1.11\,$MHz, at a gas pressure $p_{\rm g} = 4\,$mbar and total laser power $P = 1.35\,$W, and record its motion continuously for four days, as described in the Methods section. The PSD of the locked rotation is shown in Fig. 1b. We record an extremely narrow feature, which, when fit with a Lorentzian, yields a FWHM below $1.3\,\mu$Hz within one standard deviation. This gives an effective $Q_{\rm m} = f_{\rm r}/\Delta f_{\rm r}$ of 7.7×10^{11}, the highest value ever recorded for a mechanical system. In this way we achieve ultra-high stability rotations. The phase noise reaches $-80\,$dBc/Hz at only 3 mHz from the carrier frequency (Fig. 2a), and the Allan deviation shows that after four days of recording the relative frequency fluctuations are below one part in 10^{11}, which is almost as stable as the drive itself (Fig. 2b).

To explain this ultra-stable rotation, we model the dy-

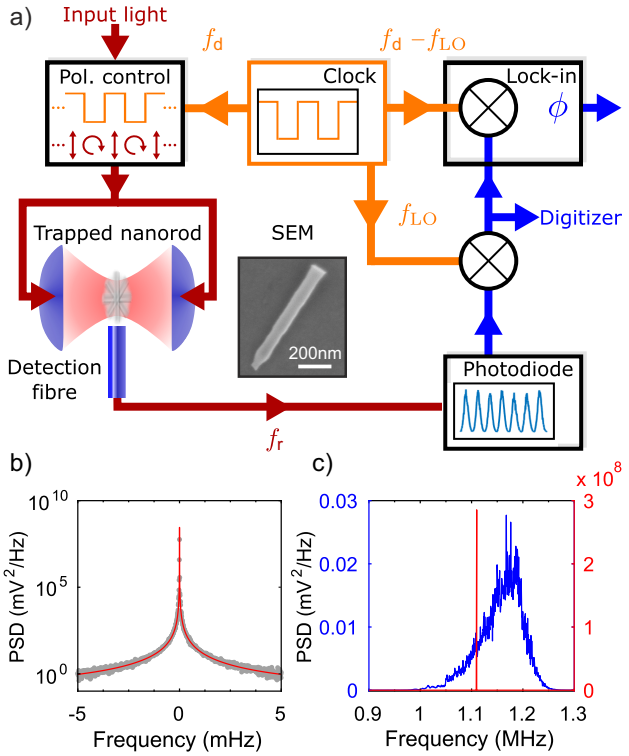

FIG. 1: Frequency locking. a) A silicon nanorod is optically trapped in a standing-wave formed by counterpropagating focussed laser beams at $\lambda = 1550\,\mathrm{nm}$, see the Methods section. The polarization of the light is controlled using a fibre-EOM driven by a signal generator. We detect the motion of the nanorod via the scattered light collected in a multimode optical fibre. The signal is mixed down with a local oscillator f_{LO} to record the spectrum and the phase of the rotation with respect to the drive frequency f_{d}. Both frequencies f_{d} and f_{LO} are synced to a common clock. b) Power spectral density (gray points) of the frequency-locked rotation at 1.11 MHz, taken over 4 continuous days, fit with a Lorentzian (red curve). The upper bound on the FWHM is $1.3\,\mu$Hz. c) Comparison of frequency-locked (red, right axis) and un-locked (blue, left axis) rotation.

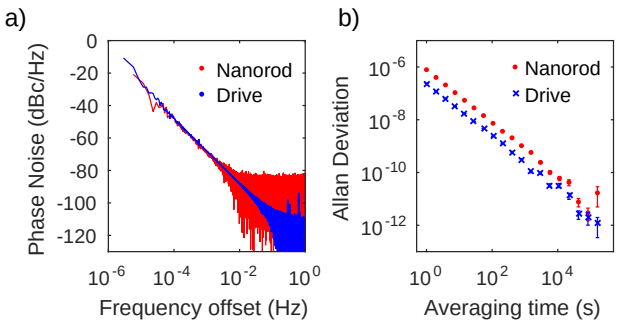

FIG. 2: Characterizing the rotations. a) The phase noise of the rotor (red) and drive (blue). b) The Allan deviation indicates that the mechanical motion (red dots) follows the stability of the drive (blue crosses) to within one order of magnitude. This leads to a long-term (4 day) frequency stability for the mechanical rotation of less than 10^{-11}.

namics of the rod's orientation α with respect to the polarization axis [8]. Denoting by Γ the damping rate due to gas collisions (a function of gas pressure p_{g}), by N the torque exerted by the circularly polarized standing wave (a function of laser power P) and by V the maximum potential energy of the rod in a linearly polarized standing wave, the equation of motion is

$$\ddot{\alpha} = -\Gamma\dot{\alpha} + \frac{N}{I}h(t) - \frac{V}{I}\sin(2\alpha)[1 - h(t)], \qquad (1)$$

where $I = M\ell^2/12$ is the moment of inertia and $h(t)$ represents the periodic driving, with $h(t) = 1$ for circular polarization at $t \in [0, 1/2f_{\mathrm{d}})$ and $h(t) = 0$ for linear polarization at $t \in [1/2f_{\mathrm{d}}, 1/f_{\mathrm{d}})$; expressions for Γ, N, and V are given in the Methods section.

In the limit of long driving times $t \gg 1/f_{\mathrm{d}}$ the nanorod rotates with constant mean rotation frequency $f_{\mathrm{r}} = \langle\dot{\alpha}\rangle/2\pi$, and its motion approaches one of two qualitatively distinct types of limit cycle. In the first type, *threshold rotation*, $f_{\mathrm{r}} = N/(4\pi I\Gamma)$ is determined by the balance between Γ and the time averaged radiation torque $N/2$. Threshold rotation exhibits a broad frequency distribution, as shown by the blue curve in Fig. 1c, due to its dependence on P and p_{g} [8].

In the second type of limit cycle, the aforementioned *locked rotation*, f_{r} locks to a rational fraction of the driving frequency. Experimentally, we observe $f_{\mathrm{r}} : f_{\mathrm{d}} = 1 : 2$ - and $f_{\mathrm{r}} : f_{\mathrm{d}} = 1 : 4$ - locking, where the rod performs one rotation in two or four driving periods, respectively. The rotational frequency f_{r} now *does not* depend on environmental parameters such as p_{g} or P, but only on the frequency stability of the drive. This allows us to achieve an exceptionally high rotational frequency stability.

The realized limit cycle is determined by the initial dynamics of the nanorod, and by experimental parameters such as $p_{\mathrm{g}}, P, f_{\mathrm{d}}$, and the rod dimensions. For a given nanorod the ratio between torque and potential is fixed, and thus Eq. (1) depends only on the dimensionless damping rate Γ/f_{d} and dimensionless torque $N/f_{\mathrm{d}}^2 I$. In Fig. 3a we show this reduced parameter space. The blue shaded area indicates the region where $1 : 2$ - locking is possible. The labelled solid lines indicate where threshold and locked rotations have the same frequency, and locking occurs independent of the initial conditions.

To explore the dynamics of the driven nanorotor, we experimentally vary p_{g} and f_{d}, thereby following a path through parameter space (red line in Fig. 3a). The observed f_{r} are shown as blue points in Fig. 3b, the top panel showing the path 1-2-3, and the lower panel 3-4. This plot shows that for certain parameters both types of limit cycles can be observed, depending on the initial conditions. When starting from 1, the rotation $1 : 2$ - locks to the drive (horizontal solid line). When increasing p_{g} along 1-2, the rod jumps out of lock, and exhibits threshold rotation. When decreasing f_{d} along 2-3, the rod remains at threshold rotation, following the theoretically

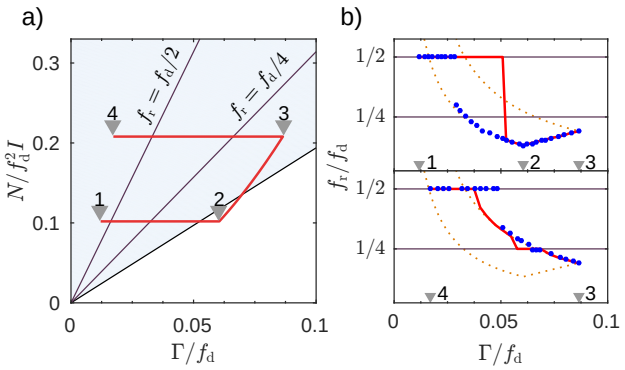

FIG. 3: Driven rotor. a) Reduced parameter space for the periodically driven nanorod. Different regions can exhibit different limit cycles, as determined by the initial conditions. Within the blue shaded region $f_r : f_d = 1 : 2$ - locking can occur, while it can not be realized in the white region. Along the labelled solid lines the frequency of threshold rotation coincides with $1 : 2$ - or $1 : 4$ - locking. To explore the various limit cycles we select a path in parameter space (solid red line) which we follow experimentally by adiabatically varying p_g and f_d. b) Experimentally measured rotation frequencies f_r along the path in parameter space (blue points), and simulation (solid red line). The three different limit cycles observed are: threshold rotation (orange dotted lines), $1 : 2$ - and $1 : 4$ - locking (horizontal solid lines).

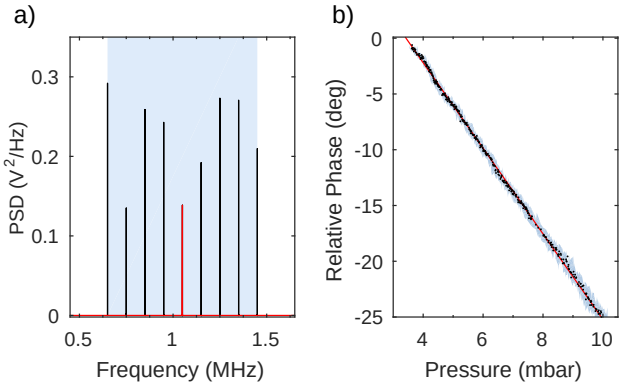

FIG. 4: Sensing applications. a) At 4 mbar, the locking frequency f_d can be continuously tuned by over 800 kHz, which corresponds to almost 10^{12} linewidths. The peaks in the PSD differ in amplitude since for short recording times they are not fully resolved. b) In this parameter region the phase lag between the oscillator and the drive depends linearly on pressure and thus can be used for precise pressure sensing. The error margin (shaded region) in this measurement is set by the resolution and repeatability of the commercial pressure gauge.

expected frequencies with excellent agreement (orange dotted lines). Decreasing p_g along 3-4, the rod first follows the threshold rotation frequency until it crosses the horizontal line, where it briefly enters $1 : 4$ - locked rotation, returns to threshold rotation and eventually jumps into $1 : 2$ - locked rotation. The solid red lines in Fig. 3b are the theoretically predicted f_r for an adiabatic path through parameter space, with the discrepancy due to imperfect adiabatic control in the experiment.

For $1 : 2$ - locked rotation, the phase lag ϕ between the drive and the rotation is

$$\phi = \arccos\left[\frac{\pi}{2V}\left(N - 2\pi f_d I \Gamma\right)\right]; \qquad (2)$$

it depends upon gas pressure p_g through Γ and on laser power P through V and N. The requirement that this phase is real defines the shaded region in Fig. 3a.

The phase ϕ can be monitored using a lock-in amplifier (see the Methods section). For a constant laser power P, measuring the phase amounts to local sensing of the gas pressure p_g, as shown in Fig. 4b. We achieve a relative pressure sensitivity of 0.3 %, which is currently limited only by the intensity noise of the fiber amplifier. This sensitivity may still be improved by five to six orders of magnitude by stabilizing the power [28]. This shows the great potential of our system as a pressure sensor. The fine spatial resolution provided by this micrometer-sized rotor allows, for instance, mapping of velocity fields and turbulences in rarefied gas flows or atomic beams.

The driven nanorod is sensitive to any externally applied torques through Eq. (1). From Eq. (2), the torque sensitivity can be estimated as 2.4×10^{-22} Nm for our current experimental parameters, which at room temperature is the highest value achieved in state of the art systems [11], and which also can be significantly improved by laser power stabilization.

A great advantage of the driven nanorotor over other high Q_m systems is the absence of an intrinsic resonance frequency. By varying f_d we can tune the frequency at ultra-high Q_m over almost 10^{12} linewidths, as shown in Fig. 4a. This unique feature makes the levitated nanorotor highly attractive for local force sensing, since in general a high Q_m naturally comes with the cost of a low bandwidth. Measuring the phase lag rather than the frequency shift allows us to monitor force variations in real time. We thus circumvent a major limitation of typical high Q_m force sensors, whose measurement time grows inherently with Q_m.

In conclusion, we have presented a novel system where polarization modulation in a standing light wave propels a levitated nanomechanical rotor at low pressures. For a wide range of experimental parameters the kicked rotor is attracted to a stable limit cycle, where the rotation frequency is locked to the external drive. When locked, the rotational frequency noise is independent of gas pressure or laser power fluctuations. This leads to a record mechanical quality factor and can be used for instantaneous, highly sensitive local measurements of pressure or torque. For instance, the current set-up allows for detection of non-conservative forces due to photon absorption or emission, shear forces in gas flows, radiation pressures in light fields, optical potentials, mass and size variations of the rod due to gas accommodation, and local pressure and temperature variations in the gas. Since there is no fixed resonance frequency, the rotational frequency

can be tuned over a range of almost 10^{12} linewidths by setting the drive frequency. Employing higher optical powers, larger duty cycles of the drive, or lower gas pressures will further increase this sensing range by a factor of more than ten, while retaining its exquisite sensitivity. By reaching ultra high vacuum this technique may also be suited to prepare quantum coherent rotational dynamics for which the unprecedentedly high $Q_{\rm m} f_{\rm r}$ product may be exploited.

Methods

Nanorod trapping. A silicon nanorod of length $\ell = (725 \pm 15)\,\mathrm{nm}$ and diameter $d = (130 \pm 13)\,\mathrm{nm}$ (with mass $M = 1.7 \times 10^{-16}\,\mathrm{kg}$) is trapped at a pressure of $p_{\rm g} = 4\,\mathrm{mbar}$, using light of total power $P = 1.35\,\mathrm{W}$ with RMS power fluctuations of 0.3%. Our method of producing and trapping the nanorods is described in Refs. [8, 29]. The motion is monitored by placing a 1 mm core multimode fibre less than $100\,\mu$m from the trapped nanorod, which collects the light that the nanoparticle scatters, yielding information about all translational and rotational degrees of freedom.

Oscillation analysis. In order to record a time series as long as 4 days we mix down the scattered light with a local oscillator at frequency $f_{\rm LO}$ such that the rotational motion signal of the rod is shifted to a frequency of 190 Hz (see Fig. 1a) and digitized with a sampling rate of 2 kS/s. This signal can then be used to calculate the Allan deviation and the phase noise $S_\phi(f) = 10\log_{10}[\mathrm{PSD}(f)/\mathrm{PSD}(f_{\rm d})]$ in units of dBc/Hz. The drive signal is recorded and analysed in the same way. To extract the relative phase of the nanorod rotation with respect to the drive we use an Stanford Research Systems lock-in amplifier (SR830) which performs a homodyne measurement on the mixed-down 190 Hz scattering signal. For this purpose both the modulation frequency $f_{\rm d}$ and the local oscillator $f_{\rm LO}$ are synced to a common clock.

Rotational dynamics. The rotational motion depends crucially on the damping rate Γ, the radiation torque N, and the laser potential V, through Eq. (1). All three quantities can be evaluated microscopically as detailed in Refs. [8, 30]. Specifically, the rotational damping rate due to diffuse reflection of gas atoms with mass $m_{\rm g}$, evaluated in the free molecular regime, is $\Gamma = d\ell p_{\rm g}\sqrt{2\pi m_{\rm g}}(6+\pi)/8M\sqrt{k_{\rm B}T}$, where T denotes the gas temperature. The optical torque exerted by a circularly polarized standing wave can be evaluated by approximating the internal polarization field according to the generalized Rayleigh-Gans approximation [30] as $N = P\Delta\chi\ell^2 d^4 k^3[\Delta\chi\eta_1(k\ell) + \chi_\perp\eta_2(k\ell)]/48cw_0^2$, where $k = 2\pi/\lambda$ is the wavenumber, $\Delta\chi = \chi_\parallel - \chi_\perp$ depends on the two independent components of the susceptibility tensor and $\eta_1(k\ell) = 0.872$ and $\eta_2(k\ell) = 0.113$ [8]. In a similar fashion, one obtains for the laser potential $V = Pd^2\ell\Delta\chi/2cw_0^2$.

* Electronic address: stefan.kuhn@univie.ac.at

[1] Aspelmeyer, M., Kippenberg, T. J. and Marquardt, F., "Cavity optomechanics." *Rev. Mod. Phys.* **86**, 1391 (2014).

[2] Chaste, J., Eichler, A., Moser, J., Ceballos, G., Rurali. R and Bachtold, A., "A nanomechanical mass sensor with yoctogram resolution." *Nature Nanotech.* **7**, 301 (2012).

[3] Schliesser, A., Arcizet, O., Riviére, R., Anetsberger, G. and Kippenberg T. J., "Resolved-sideband cooling and position measurement of a micromechanical oscillator close to the Heisenberg uncertainty limit." *Nature Phys.* **5**, 509 (2009).

[4] Teufel, J. D., Donner, T., Castellanos-Beltran, M. A., Harlow, J. W. and Lehnert, K. W., "Nanomechanical motion measured with an imprecision below that at the standard quantum limit." *Nature Nanotech.* **4**, 820 (2009).

[5] Calleja, M, Kosaka, P. M., San Paulo, A. and Tamayo, J., "Challenges for nanomechanical sensors in biological detection." *Nanoscale* **4**, 4925 (2012).

[6] Tong, L., Miljković, V. D. and Käll, M., "Alignment, Rotation, and Spinning of Single Plasmonic Nanoparticles and Nanowires Using Polarization Dependent Optical Forces." *Nano Lett.* **10**, 268-273 (2009).

[7] Arita, Y., Mazilu, M. and Dholakia, K., "Laser-induced rotation and cooling of a trapped microgyroscope in vacuum." *Nature Communs.* **4**, 2374 (2013).

[8] Kuhn, S. *et al.*, "Full Rotational Control of Levitated Silicon Nanorods." *arXiv*:1608.07315 (2016).

[9] Norte, R. A., Moura, J. P., Gröblacher, S., "Mechanical Resonators for Quantum Optomechanics Experiments at Room Temperature." *Phys. Rev. Lett.* **116**, 147202 (2016).

[10] Tsaturyan, Y., Barg, A., Polzik, E. S. and Schliesser, A., "Ultra-coherent nanomechanical resonators via soft clamping and dissipation dilution." *arXiv*:1608.00937 (2016).

[11] Kim, P. H., Hauer, B. D., Doolin, C., Souris, F. and Davis, J. P., "Approaching the standard quantum limit of mechanical torque sensing." *Nature Communs.* **7**, 13165 (2016).

[12] Metcalfe, M., "Applications of cavity optomechanics." *Appl. Phys. Rev.* **1**, 031105 (2014).

[13] Gavartin, E., Verlot, P. and Kippenberg, T. J., "A hybrid on-chip optomechanical transducer for ultrasensitive force measurements." *Nature Nanotech.* **7**, 509-514 (2012).

[14] Mamin, H. J. and Rugar, D., "Sub-attonewton force detection at millikelvin temperatures." *Appl. Phys. Lett.* **79**, 33583360 (2001).

[15] Ranjit, G., Atherton, D. P., Stutz, J. H., Cunningham, M. and Geraci, A. A., "Attonewton force detection using microspheres in a dual-beam optical trap in high vacuum." *Phys. Rev. A* **91**, 051805 (2015).

[16] Krause, A. G., Winger, M., Blasius, T. D., Lin, Q. and Painter, O., "A high-resolution microchip optomechanical accelerometer." *Nature Photonics* **6**, 768 (2012).

[17] Cleland, A. and Roukes, M., "A nanometre-scale mechanical electrometer." *Nature* **392**, 160 (1998).
[18] Hossein-Zadeh, M. and Vahala, K. J., "Observation of injection locking in an optomechanical rf oscillator." *Appl. Phys. Lett.* **93**, 191115 (2008)
[19] Villanueva, L. G. *et al.*, "A Nanoscale Parametric Feedback Oscillator." *Nano Lett.* **11**, 50545059 (2011).
[20] Coppock, J. E., Nagornykh, P., Murphy, J. P. J. and Kane, B. E., "Phase locking of the rotation of a graphene nanoplatelet to an RF electric field in a quadrupole ion trap." *Proc. SPIE 9922, Optical Trapping and Optical Micromanipulation XIII*, 99220E (2016).
[21] Ekinci, K. L. and Roukes, M. L., "Nanoelectromechanical systems." *Rev. Sci. Instrum.* **76**, 061101 (2005).
[22] Cirio, M., Brennen, G. K. and Twamley, J., "Quantum Magnetomechanics: Ultrahigh-Q-Levitated Mechanical Oscillators." *Phys. Rev. Lett.* **109**, 147206 (2012)
[23] Yin, Z.-Q., Geraci, A. A. and Li, T., "Optomechanics of levitated dielectric particles." *Int. J. Mod. Phys. B* **3**, 3244 (2014).
[24] Kiesel, N. *et al.*, "Cavity cooling of an optically levitated submicron particle." *Proc. Natl. Acad. Sci. USA* **110**, 1418014185 (2013).
[25] Millen J., Fonseca, P. Z. G., Mavrogordatos, T., Monteiro, T. S. and Barker, P. F., "Cavity Cooling a Single Charged Levitated Nanosphere" *Phys. Rev. Lett.* **114**, 123602 (2015).
[26] Hoang, T. M. *et al.*, "Torsional Optomechanics of a Levitated Nonspherical Nanoparticle." *Phys. Rev. Lett.* **117**, 123604 (2016)
[27] Gieseler, J., Novotny, L. and Quidant, R., "Thermal nonlinearities in a nanomechanical oscillator." *Nature Phys.* **9**, 806-810 (2013).
[28] Kwee, P., Willke, B. and Danzmann, K., "New concepts and results in laser power stabilization." *Appl. Phys. B* **102**, 515-522 (2011)
[29] Kuhn, S. *et al.*, "Cavity-Assisted Manipulation of Freely Rotating Silicon Nanorods in High Vacuum." *Nano Lett.* **15**, 56045608 (2015).
[30] Stickler, B. A. *et al.*, "Ro-Translational Cavity Cooling of Dielectric Rods and Disks." *Phys. Rev. A* **94**, 033818 (2016)

Acknowledgments
We are grateful for financial support by the Austrian Science Funds (FWF) in the project P27297 and DK-CoQuS (W1210-3). We acknowledge support by S. Puchegger and the faculty center for nanostructure research at the University of Vienna in imaging the nanorods. J.M. acknowledges funding from the European Unions Horizon 2020 research and innovation programme under the Marie Skłodowska-Curie grant agreement No 654532. F.P. acknowledges the Legacy Program (Israel Science Foundation) for its support.

Author Contributions
S.K., M.A. and J.M. conceived of and designed the experiment. S.K. and J.M. performed all experiments. S.K., B.A.S. and J.M. analysed the data. A.K. and F.P. fabricated the nanorods. B.A.S. and K.H. developed all theoretical models. S.K., B.A.S., K.H., M.A. and J.M. contributed to the writing of the manuscript.